

A FULL CHARGE SEPARATION OVER THE TWO SAME CHROMOPHORES IN A PHOTOSYNTHETIC TETRAD

ATSUHIRO OSUKA^{*1}, SHINJI MARUMO¹, TADASHI OKADA^{*2}, SEIJI TANIGUCHI², NOBORU MATAGA^{*3}
TAKESHI OHNO⁴, KOICHI NOZAKI⁴, IWAO YAMAZAKI⁵ and YOSHINOBU NISHIMURA⁵

¹Department of Chemistry, Kyoto University, Kyoto 606-01, Japan

²Department of Chemistry, Osaka University, Toyonaka 560, Japan

³Institute for Laser Technology, Utsubo Honmachi, Osaka 550, Japan

⁴Department of Chemistry, Osaka University, Toyonaka 560, Japan

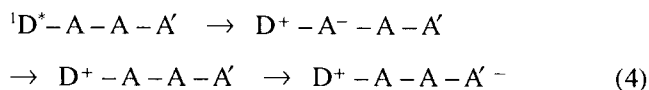
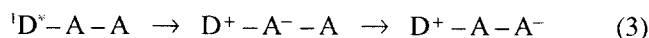
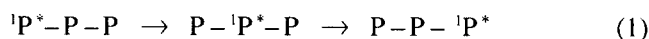
⁵Department of Chemical Process Engineering, Hokkaido University, Sapporo 060, Japan

(Received 3 July 1997; accepted 23 September 1997)

Abstract – The synthesis and excited-state dynamics are described for a tetrad (ZC – ZP – ZP – I) consisting of zinc chlorin (ZC), zinc porphyrin (ZP), zinc porphyrin (ZP), and pyromellitimide (I), which upon photoexcitation provides a fully charge-separated state (ZC⁺ – P – ZP – I⁻) with lifetimes of 230 μs in THF and > 50 μs in DMF at room temperature via a stepwise electron-transfer relay that has been detected by the ps-time resolved transient absorption spectroscopy.

INTRODUCTION

The transfer of electron, hole, and excitation energy over a repeated chromophoric array has recently attracted considerable interest. In the singlet energy transfer, energy hopping among the same chromophores leads to energetically almost the degenerate states [Eq. (1)] and thus can be effective over a large number of chromophores both in vivo and in vitro systems.^{1–4} Efficient energy transfer is vital for the antenna pigments and funnels excitation energy to the reaction center. In light-harvesting antenna system, unfavorable competing processes are radiative and nonradiative decays of each chromophore and deleterious electron-transfer quenching reactions. Similar situations may be hold for the hole transfer [Eq. (2)], as seen for recent examples such as oxidative DNA damages.^{5,6} In contrast, a full charge separation (CS) from ¹D^{*}–A–A to generate D⁺–A–A⁻ [Eq. (3)] is usually difficult, since the secondary electron transfer process, D⁺–A⁻–A → D⁺–A–A⁻, that is called a charge shift reaction (CSH), should be endothermic due to energy loss of Coulomb stabilization in the latter ion-pair and in most cases cannot compete with energy wasteful charge recombination reaction to give the ground state.⁷ This is most serious in nonpolar solvents.



It occurred to us that this inefficient CSH step may be realized in a D – A – A – A' tetrad model, in which the terminal A' is set to be a stronger electron acceptor than A, thus allowing the electron transfer step from D⁺ – A – A⁻ – A' → D⁺ – A – A – A'⁻ to be highly exothermic [Eq. (4)]. Gust and Moore have developed a remarkable photosynthetic pentad consisting of carotenoid-porphyrin-porphyrin-quinone 1-quinone 2 (C – P – P – Q₁ – Q₂), in which the central two porphyrins have the same structure.⁸ They reported that a fully charge-separated state with a lifetime of 340 μs is formed in CH₂Cl₂ with a 0.15 overall quantum yield. Considering the presence of the identical two porphyrin chromophores between the C and the Q₁, the formation of C⁺ – P – P – Q₁ – Q₂⁻ indicates that at some timing intrinsic endothermic charge-shift reactions must be overcome by subsequent exothermic charge shift reactions. They only observed the fluorescence quenching of the porphyrin subunits and the formation of the C⁺ state at 970 nm in ns-μs time scale, and the fast electron-transfer events in ps time scale still remain to be clarified by the transient absorption method.

* To whom correspondence should be addressed.

†Abbreviations used : ZC, zinc chlorin; ZP, zinc porphyrin; I, pyromellitimide; THF, tetrahydrofuran; DMF, N,N-dimethylformamide; CS, charge separation; CSH, charge shift reaction; CR, charge recombination; FAB, fast atom bombardment; IR, infrared; TFA, trifluoroacetic acid; DDQ, 2,3-dichloro-2,3-dicyano-1,4-benzoquinone.

In the supramolecular photosynthetic model studies, the detection of electron-transfer processes in real time scale becomes increasingly important since it can provide important information on the mechanism involved.⁹ But this is not necessarily possible in every photosynthetic model, since the measurement of the transient absorption spectra usually encounters many difficulties such as the lack of characteristic absorption bands of intermediates, the overlap of the absorption bands, and the mismatch of instrumental time resolution with a rate of the process concerned.

In order to achieve the sequential electron-transfer relay of Eq. (4), the following features are desirable to be incorporated into a tetrad model; 1) the terminal electron donor, ${}^1D^*$, has the lowest excitation energy than ${}^1A^*$ and ${}^1A'^*$, 2) the energy transfer from ${}^1A^*$ to D should be much faster than the electron transfer from ${}^1A^*$ to A' , 3) the electron transfer from ${}^1D^*$ to A can occur efficiently, and finally 4) the energy level of $D^+ - A - A - A'^-$ is lower enough than those of $D^+ - A^- - A - A'$ and $D^+ - A - A^- - A'$ to permit the electron-transfer relay reaching to the formation of the fully charge separated state $D^+ - A - A - A'^-$. From the spectroscopic point of view, it is also highly desirable that each key intermediate such as the excited state and the ion-pair state has respective characteristic absorption bands which facilitate the analysis of the excited-state dynamics of complicated model.

Fortunately, nearly all of these requirements are fulfilled in tetrad ZC-ZP-ZP-I (Chart 1) in which a zinc chlorin (ZC), a zinc porphyrin (ZP), and a zinc porphyrin (ZP) are linked with a 1,4-phenylene space in a linear manner and a pyromellitimide(I) moiety is linked to the terminal ZP with a -phenyl-CH₂- spacer. Recently, we have developed triad ZC-ZP-I which gives a fully charge-separated state, $ZC^+ - ZP - I^-$, via a pre-formed equilibrium between ${}^1ZP^* - ZP - I$ and $ZP^+ - ZP^- - I$ followed by a rapid CSH.¹⁰ In ZC-ZP-I, the energy level of ${}^1ZC^*$ (2.13 eV) is distinctly lower than that of ${}^1ZP^*$ (1.94 eV) and the singlet energy transfer from the latter to the former is very rapid (ca. $4 \sim 6 \times 10^{10} s^{-1}$). The similar energy transfer can be expected in ZC-ZP-ZP-I. Finally, it is interesting to note that key ionic species such as ZP^- and I^- have characteristic absorption bands around 883 and 715 nm,^{10,11}

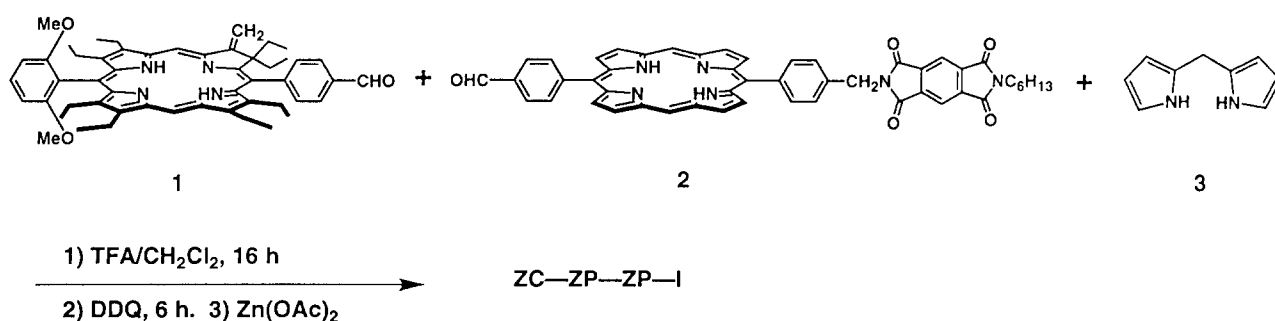
respectively, which are very useful for tracing the electron-transfer dynamics. Here we report the synthesis and photoexcited dynamics of ZC-ZP-ZP-I.

MATERIALS AND METHODS

General Procedures. 1H -NMR spectra were recorded on a JEOL α -500 spectrometer (operating as 500 MHz) and chemical shifts (δ) were reported in ppm with $CHCl_3$ as an internal standard. Ground state absorption measurements were made on a Shimadzu UV-2400PC spectrometer and steady-state fluorescence spectra were taken on a Shimadzu RF-5300PC spectrofluorophotometer specially equipped with a Hamamatsu R928 photomultiplier to measure corrected fluorescence spectra up to 900 nm. High resolution mass spectra were recorded on a JEOL HX-110 mass spectrometer. Polyethyleneglycol and CsI were used as the internal standards. 3-Nitrobenzyl alcohol was used as the FAB matrix, and the positive FAB ionization method was used at accelerating voltage 10kV with Xe atom as the primary ion source. IR spectra (KBr method) were taken on a HORIBA FT-3000 spectrometer.

Fluorescence lifetimes were measured on $10^{-7} M$ air-saturated solutions with a picosecond time-correlated single-photon counting system.¹² Picosecond transient absorption spectra were measured by means of a microcomputer-controlled double-beam picosecond spectrometer with a picosecond dye laser 8-ps pulse duration pumped by the second harmonic of a repetitive mode-locked Nd:YAG laser.¹³ The second harmonic of the Nd:YAG laser pulse or the 620 nm output of the dye laser was used for excitation. A Q-switched Nd:YAG laser (Quantel YG580) with the second harmonic output (532 nm, 15 ns pulse duration) of 40 mJ was used for measurements of nanosecond transient absorption spectra.¹⁴

Synthesis of ZC-ZP-ZP-I. Pyromellitimide-bearing formyl substituted porphyrin **2**¹⁰ (32 mg, 40 μ mol) was dissolved in 30 mL of dry CH_2Cl_2 . After confirming all the porphyrin was dissolved, formyl substituted chlorin **1**¹⁵ (48 mg, 61 μ mol) and dipyrromethane **3** (15 mg, 100 μ mol) were added to the above solution. Then 20 mL of dry CH_2Cl_2 was added and the condensation reaction was started by addition of TFA (8 μ L). The mixture was stirred for 16 h at room temperature under N_2



Scheme 1. Synthesis of ZC-ZP-ZP-I tetrad.

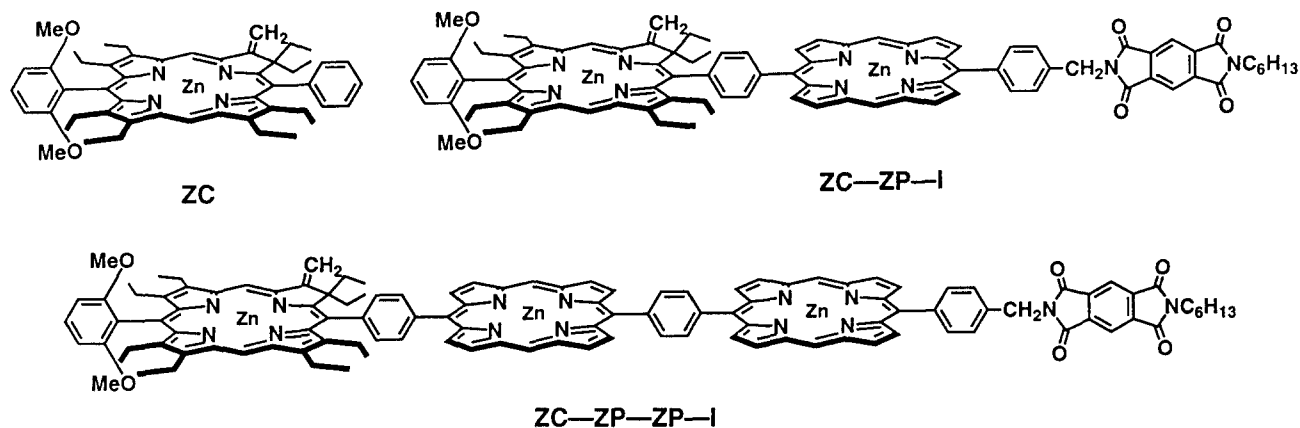
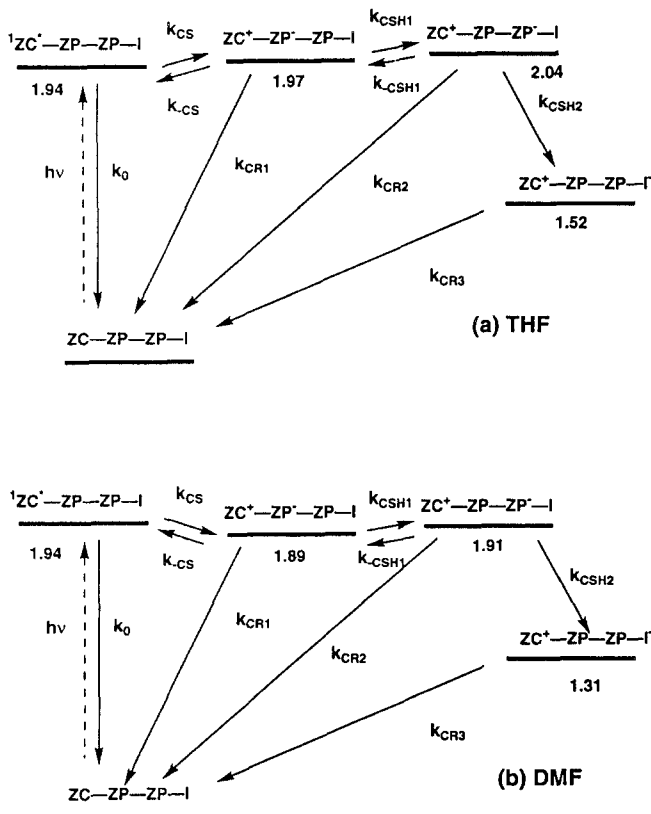


Chart 1. Structures of the models studied in this paper.

atmosphere in the dark. DDQ (34 mg, 0.15 μmol) was added, and the resulting solution was stirred for an additional 6 h. The reaction was quenched with triethylamine (0.5 mL). After evaporation of the solvent, the residue was separated by flash column chromatography on silica gel (CH_2Cl_2 eluent). The brown band was collected and the solvent was evaporated. Recrystallization from CH_2Cl_2 /hexane gave a tetrad in all free-base form which was transformed into ZC-ZP-ZP-I by treatment with $\text{Zn}(\text{OAc})_2$. After flash column chromatography,

ZC-ZP-ZP-I was obtained as dark solids (15 mg, 12% on the basis of the amount of **2** used). ^1H NMR (CDCl_3) 0.68 (t, 6H, rearranged- CH_2CH_3), 0.88 (t, 3H, N-hexyl-Me), 1.11 (t, 3H, $J=7.3$ Hz, CH_2CH_3), 1.26-1.90 (m, 6H, N-hexyl- CH_2), 1.56 (m, 2H, N-hexyl- CH_2), 1.64 (t, 3H, $J=7.3$ Hz, CH_2CH_3), 1.76 (t, 3H, $J=7.3$ Hz, CH_2CH_3), 1.80 (t, 3H, $J=7.3$ Hz, CH_2CH_3), 1.93 (t, 3H, $J=7.3$ Hz, CH_2CH_3), 2.1-2.2 (m, 2H, rearranged- CH_2CH_3), 2.8 (m, 2H, rearranged- CH_2CH_3), 2.85-2.95 (m, 4H, CH_2CH_3), 3.15 (m, 2H, CH_2CH_3), 3.45 (t, 2H, $J=7.3$ Hz, N-hexyl- CH_2), 3.60 (s, 6H, OMe), 3.76-3.85 (m, 4H, CH_2CH_3), 4.00 (m, 2H, CH_2CH_3), 5.15 (s, 2H, benzyl- CH_2), 5.67 (s, broad, 1H, methylene-H), 6.94 (s, broad, 1H, methylene-H), 6.95 (d, 2H, $J=8.5$ Hz, Ar-H), 7.74 (t, 1H, $J=8.5$ Hz, Ar-H), 7.86 (m, 4H, broad, $2 \times$ Ar-H and $2 \times$ Im-Ar-H), 8.25 (m, 2H, broad, Ar-H), 8.45 (d, 2H, $J=7.9$ Hz, Ar-H), 8.50 (d, 2H, $J=7.9$ Hz, Ar-H), 8.70 (m, 2H, broad, Ar-H), 9.05 (m, 2H, broad, Por- β -H), 9.29 (m, 2H, broad, Por- β -H), 9.40 (s, 1H, Chl-meso-H), 9.46 (d, 2H, $J=3.4$ Hz, Por- β -H), 9.50 (m, 2H, broad, Por- β -H), 9.6-9.7 (m, 8H, broad, Por- β -H), 9.76 (s, 1H, Chl-meso-1H), 10.15 (s, 1H, broad, Por-meso-H), 10.19 (s, 1H, broad, Por-meso-H), 10.33 (s, 1H, broad, Por-meso-H), and 10.37 (s, 1H, broad, Por-meso-H). HRMS(FAB): found, m/z 2032.5967; calcd. for $\text{C}_{120}\text{H}_{102}\text{N}_{14}\text{O}_6\text{Zn}_3$, m/z 2032.5981 (M^+). IR(KBr) ν_{max} : 1606 cm^{-1} (methylene- CH_2) and 1720 cm^{-1} (CO). UV(THF), peak top (relative ϵ) 404.5 (0.615), 422 (0.680), 433 (1.0), 544.5 (0.076), 585 (0.029), and 636 (0.074).



Scheme 2. Photoexcited reaction scheme of ZC-ZP-ZP-I; a) in THF, b) in DMF. Numbers below the respective states indicate the energy levels (eV).

RESULTS AND DISCUSSION

Synthesis

The tetrad ZC-ZP-ZP-I was prepared *via* the TFA promoted condensation of formyl-substituted chlorin **1**¹⁰ and formyl-substituted I-bearing porphyrin **2**¹⁵ with dipyrromethane **3** followed by oxidation with DDQ and final zinc insertion with $\text{Zn}(\text{OAc})_2$ (Scheme 1). Separation of the products by flash column chromatography over silica gel gave ZC-ZP-ZP-I with a 12%

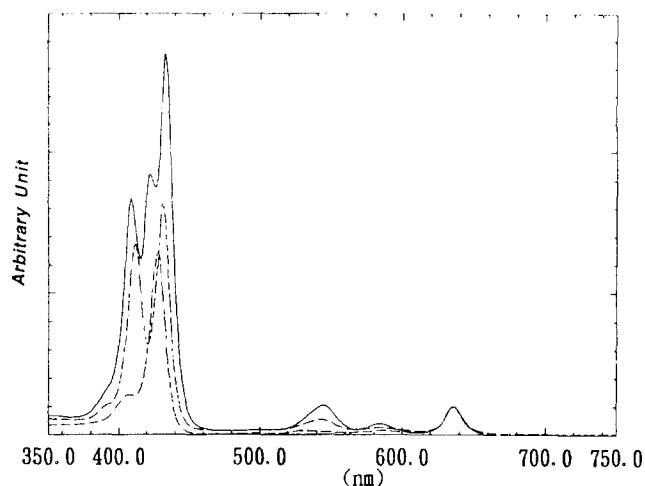


Figure 1. UV-visible absorption spectra of ZC (---), ZC-ZP-I (-·-), and ZC-ZP-ZP-I (—) in THF.

overall yield on the basis of the amount of **2** used. The structure of ZC-ZP-ZP-I was fully characterized by 500 MHz $^1\text{H-NMR}$ and FAB mass measurements. The $^1\text{H-NMR}$ spectrum indicates the meso protons appearing at δ 9.40 ppm (s, 1H, ZC), 9.76 (s, 1H, ZC), 10.15 (s, 1H, ZP), 10.19 (s, 1H, ZP), 10.33 (s, 1H, ZP), and 10.37 (s, 1H, ZP) and the exo-methylene protons appearing at δ 5.67 (s, 1H) and 6.94 ppm (s, 1H), and the high resolution mass spectrum indicates its exact mass at m/e 2032.5967; calcd for $\text{C}_{120}\text{H}_{102}\text{N}_{14}\text{O}_6\text{Zn}_3$ at m/e 2032.5981

Energetics

The energy diagram is summarized in Scheme 2. The energies of the excited states and ion pair states are determined by the method used in the previous paper.¹⁰ Following features are important, 1) the charge separation (CS) from $^1\text{ZC}^*-\text{ZP}-\text{ZP}-\text{I} \rightarrow \text{ZC}^+-\text{ZP}^--\text{ZP}-\text{I}$ is slightly endothermic in THF and exothermic in DMF; 2) the initial charge shift reaction (CSH1) of $\text{ZC}^+-\text{ZP}^--\text{ZP}-\text{I} \rightarrow \text{ZC}^+-\text{ZP}-\text{ZP}^--\text{I}$ is endothermic both in THF and DMF due to a loss of electrostatic energy, while the secondary charge shift reaction (CSH2) of $\text{ZC}^+-\text{ZP}-\text{ZP}^--\text{I} \rightarrow \text{ZC}^+-\text{ZP}-\text{ZP}-\text{I}^-$ is a highly exothermic reaction. In the charge separation in multi-chromophoric arrays, the competition between CSH1 reaction and CRI reaction is often critical in determining the quantum yield of long-distance charge separation. Thus, the endothermic CSH1 in ZC-ZP-ZP-I is unfavorable for achieving high-yield charge separation.

Absorption Spectra

The absorption spectrum of ZC-ZP-ZP-I in THF was shown in Fig. 1 along with those of ZC-ZP-I and the reference zinc chlorin (ZC). The reference ZC exhibits the Soret band at 427.5 nm and the Q-bands at

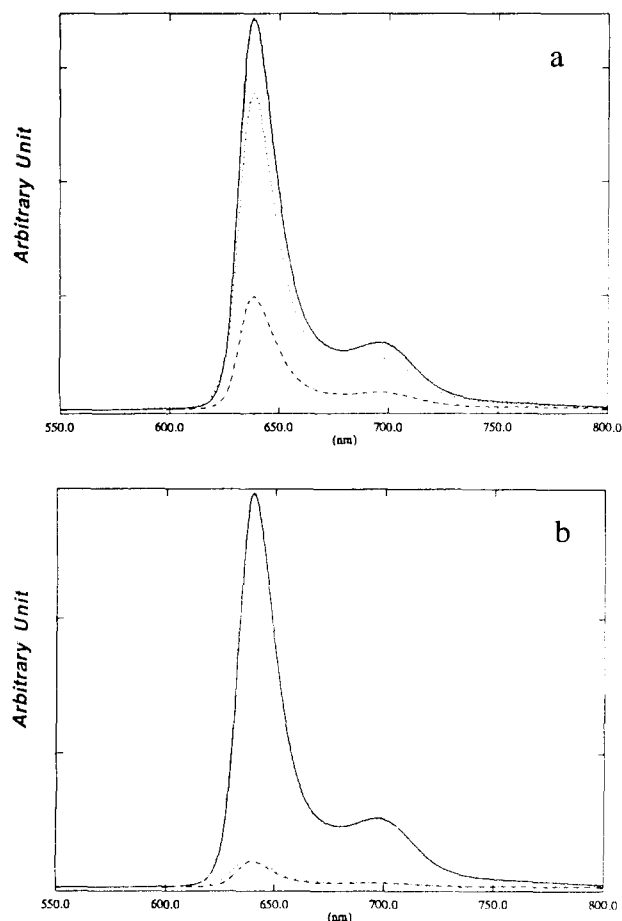


Figure 2. Steady-state fluorescence spectra of ZC (—), ZC-ZP-I (---) and ZC-ZP-ZP-I (-·-) taken for excitation at their ZC Soret bands. The absorbances at these bands are adjusted to be 1.0. (a) In THF, the excitation wavelength is 428, 432 and 434 nm, respectively. (b) In DMF, the excitation wavelength is 429, 433 and 435 nm, respectively.

530.5, 586, and 635.5 nm, and the reference zinc porphyrin monomer (ZP) exhibits the Soret band at 411 nm and the Q-bands at 542.5 and 578.5 nm (not shown), while the triad ZC-ZP-I displays the Soret bands at 411.5 (ZP) and 431 (ZC) nm and the Q-bands at 543 (ZP), 585 (ZC), and 636 (ZC) nm. The absorption spectrum of ZC-ZP-I in the Q-band region can be described as a simple sum of the respective chromophores but slight red-shifts are observed in the Soret bands. The tetrad ZC-ZP-ZP-I displays the Soret bands at 408.5, 422, and 433 nm and the Q-bands at 544.5, 585, and 636 nm. The absorption spectrum in the Q-band region are also described as the simple sum of the respective chromophores, and thus the assignment is straightforward; 544.5 nm band is due to the ZP and 585 nm and 636 nm bands are due to the ZC, while the absorption spectrum in the Soret band-region seems to indicate the exciton coupling between the two ZP subunits (408.5 and 422 nm) and relatively unperturbed band due to the ZC (433 nm). The tetrad ZC-ZP-ZP-I displays essentially the

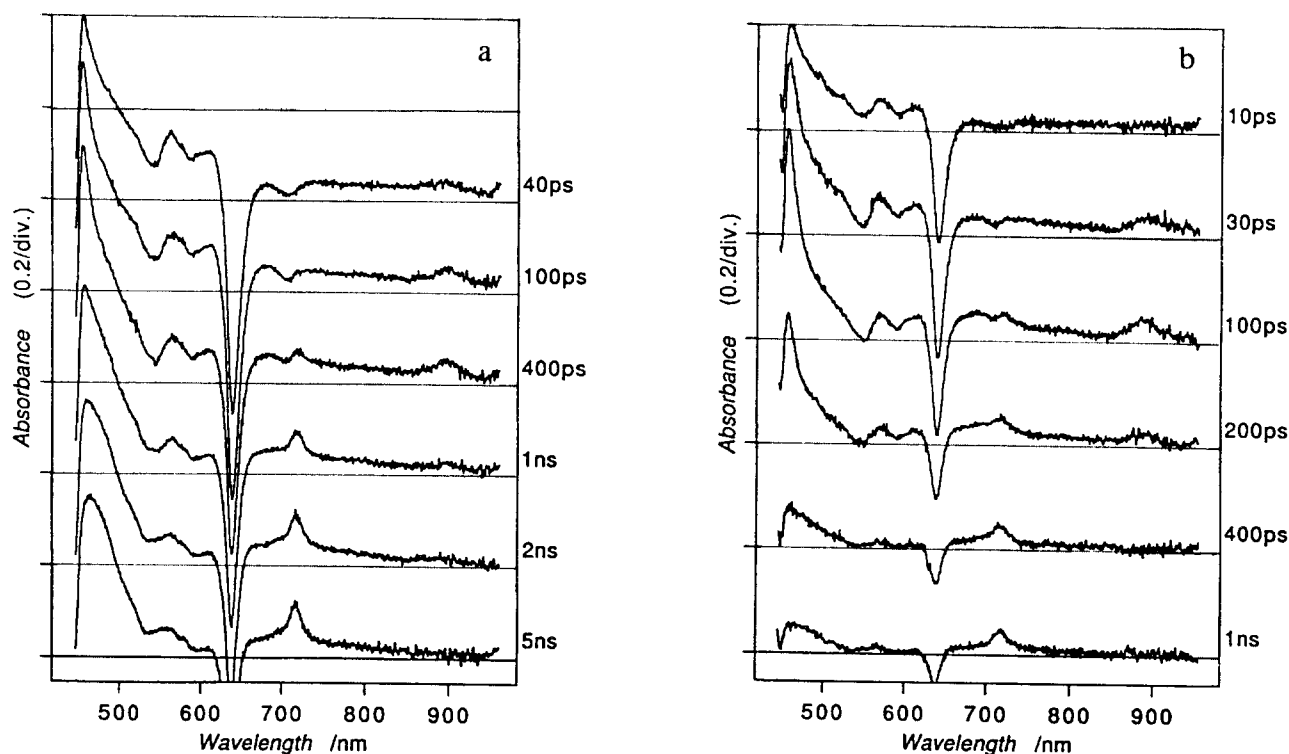


Figure 3. Time-resolved transient absorption spectra of ZC-ZP-ZP-I taken for excitation at 635 nm. (a) In THF, (b) in DMF.

same absorption spectrum in DMF (the Soret bands at 411(ZP) and 423 (ZP), and 435 (ZC) nm, and the Q-bands at 547 (ZP), 587 (ZC), and 638 (ZC) nm) with that in THF. Strong exciton coupling between a pair of two resonant zinc porphyrins bridged by a 1,4-phenylene spacer has been observed in the related models,^{4,16} while the energy levels of the ZC and the ZP are nonresonant, leading to negligible exciton coupling. Thus, as in the case for ZC-ZP-I, it is suggested that in the S_1 -states the electronic interactions between the three pigments are very weak, while in the S_2 -state the electronic interactions are modest between the ZC and ZP and rather strong between the two resonant ZP's.

Fluorescence Spectra

In the steady-state fluorescence spectra of ZC-ZP-I and ZC-ZP-ZP-I, only the emission from ZC is observed (Fig. 2). The emission peak bands of the ZC in ZC-ZP-I and ZC-ZP-ZP-I are observed at 638 nm, being ca. 2 nm blue-shifted from that of the reference ZC. The relative fluorescence intensities of ZC, ZC-ZP-I, and ZC-ZP-ZP-I which have been measured by exciting at the respective ZC Soret bands, are 1.0, 0.28, and 0.79 in THF, and 1.0, 0.07, 0.08 in DMF.

Photoexcited Dynamics

Photoexcited dynamics of ZC-ZP-ZP-I in THF is first described. The fluorescence of ZC-ZP-ZP-I

measured at 590 nm where the fluorescence is due mainly to the ZP subunits displays a single exponential decay with $\tau = 20$ ps, indicating a rapid intramolecular singlet-singlet energy transfer from the ZP-ZP subunit to the ZC subunit as is the case for ZC-ZP-I.¹⁰ Fig. 3a shows the transient absorption spectra of ZC-ZP-ZP-I taken for a selective excitation at the ZC with 635nm light. The spectrum at 40 ps delay time shows the absorption bands at 456 and 890 nm that are both due to ZP⁻. The 890nm absorption band rises with $\tau = 100$ ps and decays with $\tau = 800$ ps, which is followed by the appearance of the 717nm absorption band due to I⁻ with $\tau = 800$ ps, clearly indicating a stepwise electron transfer relay leading to a fully charge separated state, ZC⁺-ZP-ZP-I⁻. This contrasts to the result reported for ZC-ZP-I where ZC⁺-ZP⁻-I is rather difficult to be detected.¹⁰ The quantum yield for the formation of ZC⁺-ZP-ZP-I⁻ is estimated to be 0.34 on the basis of the absorbance ratio of the initial excited state ($abs_{456} = 0.27$; $\epsilon_{456} = 3.9 \times 10^4 \text{ M}^{-1}$) and the final ion pair ($abs_{717} = 0.12$; $\epsilon_{717} = 5.1 \times 10^4 \text{ M}^{-1}$). Another interesting observation is a red-shift of the absorption peak of ZP⁻ from 453 nm in ZC-ZP-I to 456 nm in ZC-ZP-ZP-I (Fig. 4). This shift may indicate the formation of ZC⁺-ZP-ZP-I, since it is plausible that the ZP⁻ subunit in ZC⁺-ZP-I and that in ZC⁺-ZP-ZP-I suffer different electric-field effect of the ZC⁺, leading to the observed shift.¹⁷ Analogous shift was also observed in related dimer-monomer-I triads having different

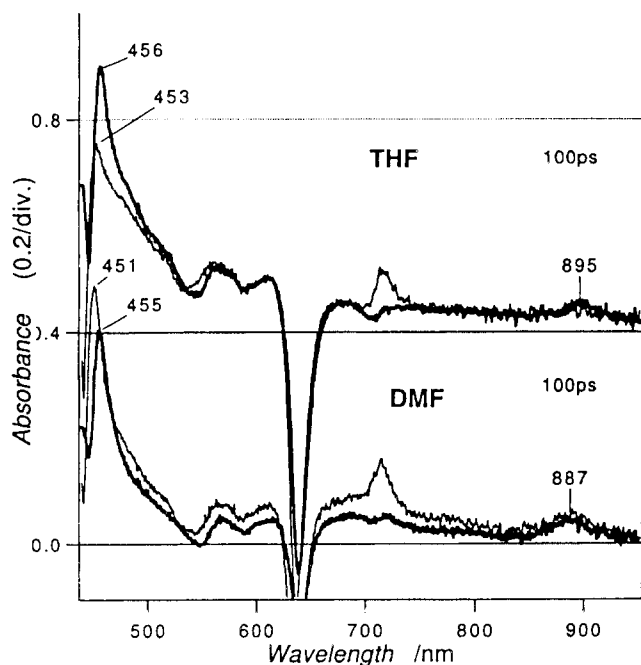


Figure 4. Time-resolved transient absorption spectra of ZC-ZP-I (—) and ZC-ZP-ZP-I (---) at 100-ps delay time in THF (upper) and DMF (lower).

spacers between the dimer and monomer.¹⁵ Based on these observations, a stepwise electron-transfer relay can be depicted as shown in Scheme 2. The fluorescence at 650 nm where the emitting species is solely the ZC exhibits biexponential decay; 55 ps (42%) and 721 ps (58%). This fluorescence decay behavior can be interpreted in terms of thermal repopulation of $^1\text{ZC}^*$ from $\text{ZC}^+ - \text{ZP}^- - \text{ZP} - \text{I}$ as is the case for $\text{ZC} - \text{ZP} - \text{I}$.^{10,18} These decay data have been analyzed on the assumption that k_{CSH1} and k_{CR2} are much smaller than highly exothermic k_{CSH2} , giving estimates of the rate constants, $k_{\text{CS}} = 7.1 \times 10^9 \text{ s}^{-1}$, $k_{\text{CS}} = 9.6 \times 10^9 \text{ s}^{-1}$, and $k_{\text{CR1}} + k_{\text{CSH1}} = 1.6 \times 10^9 \text{ s}^{-1}$, respectively. Finally, the lifetime of the resultant $\text{ZC}^+ - \text{ZP}^- - \text{ZP} - \text{I}$ has been determined by ns- μs time resolved transient absorption spectroscopy to be 230 μs at room temperature, being comparable to the pentad-lifetime reported by Gust and Moore.⁸ These results are interestingly compared with the data of $\text{ZC} - \text{ZP} - \text{I} : \Phi(\text{ZC}^+ - \text{ZP}^- - \text{I}^-) = 0.90$ and the decay of $\text{ZC}^+ - \text{ZP}^- - \text{I}^-$ to the ground state follows a biexponential function with $\tau = 130 \text{ ns}$ (70%) and 370 ns (30%).¹⁰ Thus, incorporation of an additional ZP subunit leads to a *ca.* 10^4 times increase in the lifetime of the charge separated state with a concurrent one-third decrease of the quantum yield.

In more polar DMF solution, essentially the same stepwise electron-transfer relay was observed in a much faster time scale (Fig. 3b). Namely the 890nm absorption band rises with $\tau = 50 \text{ ps}$ and decays with $\tau = 110 \text{ ps}$, and

the 717nm absorption band increases with $\tau = 110 \text{ ps}$, indicating a *ca.* 7 times faster formation of $\text{ZC}^+ - \text{ZP}^- - \text{ZP} - \text{I}^-$ in DMF. The quantum yield is 0.30 and its lifetime is $>50 \mu\text{s}$, while $\text{ZC} - \text{ZP} - \text{I}$ gives $\text{ZC}^+ - \text{ZP}^- - \text{I}^-$ in 0.48 quantum yield and the lifetime of charge-separated state is 240 ns.¹⁰

CONCLUSION

In summary, we have demonstrated that a selective excitation into $^1\text{ZC}^* - \text{ZP}^- - \text{ZP} - \text{I}$ eventually leads to the formation of $\text{ZC}^+ - \text{ZP}^- - \text{ZP} - \text{I}^-$ through a stepwise electron-transfer relay. The key endothermic CSH1 process is indeed overcome in both the solvents, probably with aid of large stabilization of the subsequent, secondary CSH2 reaction. In other words, long-distance electron transfer across multi-chromophoric array consisting of the same chromophore would be possible by making the final electron transfer to be sufficiently exothermic.

Acknowledgement – This work was partially supported by Grant-in-Aids for Scientific Research (No. 09440217 and 08874074) from the Ministry of Education, Science, Sports and Culture of Japan and by The Sumitomo Foundation and by Kansai Research Foundation for technology promotion.

REFERENCES

1. Pullerits, T. and V. Sundrom (1996) Photosynthetic light-harvesting pigment-protein complexes: toward understanding how and why. *Acc. Chem. Res.* **29**, 381-389.
2. Prathapan, S., T. E. Johnson, J. S. Lindsey (1993) Building-block synthesis of porphyrin light-harvesting arrays. *J. Am. Chem. Soc.* **115**, 7519-7520.
3. Officer, D. L., A. K. Burrell, D. C. W. Reid (1996) Building large porphyrin arrays: pentamers and nonamers. *J. Chem. Soc., Chem. Commun.*, 1657-1658.
4. Osuka, A., N. Tanabe, S. Nakajima and K. Maruyama (1996) Synthesis of 1,4-phenylene-bridged linear porphyrin arrays. *J. Chem. Soc., Perkin Trans.* **2**, 199-203.
5. Sugiyama, H. and I. Saito (1996) Theoretical Studies of GG-specific photocleavage of DNA via electron transfer: significant lowering of ionization potential and 5'-localization of HOMO of stacked GG bases in B-form DNA. *J. Am. Chem. Soc.* **118**, 7063-7068.
6. Hall, D. B., R. E. Holmlin and J. K. Barton (1996) Oxidative DNA damage through long-range electron transfer. *Nature* **382**, 731-735.
7. Kotani, S., H. Miyasaka and A. Itaya (1995) Formation of extremely long-lived charge-separated state following photoinduced electron transfer in poly(N-vinylcarbazole) coadsorbed with 1,2,4,5-tetracyanobenzene on a macroreticular resin. *J. Phys. Chem.* **99**, 13062-13064.

8. Gust, D., T. A. Moore, A. L. Moore, S.-L. Lee, E. Bittersmann, D. K. Luttrull, A. A. Rehms, J. M. DeGraziano, X. C. Ma, F. Gao, R. E. Belford and T. T. Trier (1990) Efficient multistep photoinduced electron transfer in a molecular pentad. *Science* **248**, 199-201.
9. Wasielewski, M. R. (1992) Photoinduced electron transfer in supramolecular systems for artificial photosynthesis. *Chem. Rev.* **92**, 435-461.
10. Osuka, A., S. Marumo, N. Mataga, S. Taniguchi, T. Okada, I. Yamazaki, Y. Nishimura, T. Ohno and K. Nozaki (1996) A stepwise electron-transfer relay mimicking the primary charge separation in bacterial photosynthetic reaction center. *J. Am. Chem. Soc.* **118**, 155-168.
11. Osuka, A., S. Nakajima, K. Maruyama, N. Mataga, T. Asahi, I. Yamazaki, Y. Nishimura, T. Ohno and K. Nozaki (1993) 1,2-Phenylene-bridged diporphyrin linked with porphyrin monomer and pyromellitimide as a model for photosynthetic reaction center: synthesis and photoinduced charge separation. *J. Am. Chem. Soc.* **115**, 4577-4589 (1993).
12. Yamazaki, I., N. Tamai, H. Kume, H. Tsuchiya, K. Oba (1985) Microchannel-plate photomultiplier applicability to the time-correlated photon-counting method. *Rev. Sci. Instrum.* **56**, 1187-1194.
13. Hirata, Y. and N. Mataga (1991) Direct observation of electron-cation geminate pair produced by picosecond laser pulse excitation in nonpolar solvent: excitation wavelength dependence of the electron thermalization length. *J. Phys. Chem.* **95**, 1640-1644.
14. Nozaki, K., T. Ohno and M. Haga (1992) Intramolecular electron transfer in photoexcited Ru(II)-Rh(III) binuclear compounds. *J. Phys. Chem.* **96**, 10880-10888.
15. Osuka, A., S. Nakajima, T. Okada, S. Taniguchi, K. Nozaki, T. Ohno, I. Yamazaki, Y. Nishimura and N. Mataga (1996) A sequential electron-transfer relay in diporphyrin-porphyrin-pyromellitimide triads analogous to that in the photosynthetic reaction center *Angew. Chem., Int. Ed. Engl.* **35**, 92-94.
16. Osuka, A. and K. Maruyama (1988) Synthesis of naphthalene-bridged porphyrin dimers and their orientation dependent excitation coupling. *J. Am. Chem. Soc.* **110**, 4454-4456.
17. Gosztola, D., H. Yamada and M. R. Wasielewski (1995) Magnetic field effects of photogenerated ion pairs on nearby molecules: a model for the carotenoid band shift in photosynthesis. *J. Am. Chem. Soc.* **117**, 2041-2048
18. Heitele, H., P. Finckh, S. Weeren, F. Pollinger and M. E. Michel-Beyerle (1989) Solvent polarity effects on intramolecular electron transfer. 1. Energetic aspects. *J. Phys. Chem.* **93**, 5173-5179.